Front and back side SIMS analysis of boron-doped delta-layer in diamond

M. A. Pinault-Thaury, F. Jomard, Christine Mer-Calfati, Nicolas Tranchant, Michal Pomorski, Philippe Bergonzo, Jean-Charles Arnault

Front and back side SIMS analysis of boron-doped delta-layer in diamond

M.-A. Pinault-Thaury*[1], F. Jomard[1], C. Mer-Calfati[2], N. Tranchant[2], M. Pomorski[2], P. Bergonzo[2], J.-C. Arnault[2]

[1]Groupe d'Etude de la Matière Condensée, CNRS, University of Paris Saclay, University of Versailles St Quentin, 45 Avenue des Etats-Unis, 78035 Versailles cedex, France

[2]CEA, LIST, Diamond Sensors Laboratory, 91191 Gif-sur-Yvette, France

* Corresponding author: marie-amandine.pinault-thaury@uvsq.fr

Abstract

Nowadays the availability of very thin diamond layers in the range of nanometers as well as the possibility to characterize such delta-layer structures are required for the field of photonics and spintronics, but also for the development of next generation high power devices involving boron doping. The fabrication of diamond structures with abrupt interfaces such as superlattices and quantum wells has been recently improved. A very accurate characterization is then essential even though the analysis of such structures is arduous and challenging. SIMS analyses are commonly used to obtain depth profiles of dopants. However, below 10 nm in thickness, SIMS induced ion mixing effects which are no longer negligible. Then the raw SIMS profile might differ from the real dopant profile. In this study, we have analyzed a diamond structure containing a thin boron epilayer, especially synthetized to achieve SIMS analysis on both sides and to overcome the effects of ion mixing. We evidence the ion mixing induced by primary ions. Such a structure is a delta diamond layer, comparable to classical boron-doped delta-layer in silicon. Our results show that the growth of boron-doped delta-layer in diamond is now well controlled in terms of thickness and interfaces.

Keywords

Both sides SIMS analysis; backside; depth profiling; ion mixing; diamond; boron-doped delta-layer

1. Introduction

Due to its unusual physical and chemical properties, diamond is a promising material for many applications related to color centers with nitrogen-vacancy centers [1-4] in the field of photonics and spintronics, as well as to high breakdown voltage / high temperature electronic devices [5, 6] in the development of next generation high power devices based on boron doping. During the last ten years, an intensive work was performed on its physical properties and its synthetic growth by chemical vapour deposition (CVD). The improvement in diamond epitaxy allows growing ultra-thin boron doped structures and achieving diamond MESFET fabrication [7, 8]. Such structures consist in a nanometric layer of highly boron doped diamond (P+ layer with [B] > $5x10^{20}$ at/cm^3) sandwiched between two low boron doped diamond layers (P- layers with [B] ~ $1x10^{16}$ at/cm^3). The challenge to achieve such multilayer structure is related to the growth of the P+ layer as thin as possible (around 2 nm) and to controlled sharpness of both P+/P- interfaces. According to simulations, this may allow carriers delocalization within P- layers which should lead to higher mobility [9]. Nevertheless, electrical characterizations of such boron-doped delta-layers in diamond structures didn't show mobility enhancement by confinement [10].

Such P- / P+ / P- multilayers were initially obtained by insertion of a boron rod in the CVD plasma ball [11, 12]. However, the reproducibility of this method was perfectible. More recently, this multilayer structure was achieved thanks to a precise control of the diamond growth rate at high boron doping level and to the in situ etching process with oxygen [3]. Another method, used in this study, is based on an injection system developed to shorten the residence time of active species during CVD growth [13]. As a result, several groups are currently able to grow excellent and reproducible thin heavily boron doped diamond layers surrounded by P- layers [10, 14, 15].

The SIMS analysis provides the depth distribution of the boron concentration. SIMS measurements are usually performed from the front side of the sample: the sputtering goes from the sample surface to the substrate. When the layer is very thin, typically lower than 10 nm, a broadening effect of SIMS profiles cannot be neglected due to the interactions between incident ions and the studied material. Indeed, ion mixing and roughness effects led to artefacts in SIMS profiles such as asymmetry and broadening [16, 17]. This is inherent to the SIMS technique.

In this work, we compare the SIMS profiles of the boron concentration from the front and back sides of a boron-doped delta-layer in diamond sample using SIMS parameters commonly used for diamond. We focus on artefacts occurring during SIMS analysis: ion mixing and roughness effects. The present study allows to highlight the limitations of SIMS measurements to characterize nanometric doped layers. Some previous studies performed on boron-doped silicon samples show the effectiveness of back side SIMS analysis [18-20]. It appears that combination of front and back side SIMS depth profiling can help to exclude ion beam induced atomic mixing. Such analysis provides sharp dopant distribution profiles suitable for analysing ultra-shallow layers. Thereby front and back sides SIMS analysis should allow the identification of the broadening effects and a more accurate description of the dopant distribution profile.

2. Experimental procedure

2.1. Boron-doped delta-layer in diamond sample

The diamond sample was realized in five steps (see figure 1).

Firstly (figure 1a), a 3x3x0.5 mm^3 (100) type Ib HPHT diamond substrate is implanted with oxygen ions (3 MeV with 10^{17} ions/cm^2 dose [21, 22]). This implantation creates a graphitized zone localized at a depth of 2 µm from the substrate surface as confirmed by 2D confocal Raman spectroscopy (not shown here). After conventional chemical cleaning, the substrate is introduced in a metallic CVD reactor.

The second step (figure 1b) consists in growing the diamond boron-doped delta-layer structure by microwave plasma CVD. The gas mixture is composed of methane (CH_4), hydrogen (H_2), trimethylboron (TMB). In the case of the P- layer, oxygen is added to the gas phase to decrease boron content below $5x10^{16}$ at/cm^3 [23]. For the P+ layer, a new injection system has been developed in the CVD reactor to incorporate the gas mixture in the vicinity of the diamond substrate. This innovative configuration permits to obtain high boron content up to $3x10^{20}$ at/cm^3 and very sharp interfaces between the P+ and P- layers [13]. The growth temperature, the pressure and the microwave power were fixed at 850°C, 120 mbar and 600W, respectively. The substrate temperature is measured by a pyrometer (disappearance of filament). The growth parameters and the sample characteristics are summarized in Table 1. After the second step, SIMS measurements were performed on the front side of the sample, just after the growth of the delta-layer structure.

For handling purpose, the sample is thickened (see figure 1c). As third step, a 30 µm undoped diamond layer is grown on the top of the delta-layer structure. The fourth step consists in the lift-off of the substrate (figure 1d). It is achieved using bipolar (called Marchywka effect [24]) electrochemical etching method in the implanted region on the edges of the diamond

substrate. The sample is placed in ultra-pure water between two platinum rod-electrodes. The etching process is realized by applying a high voltage (700V -1000V). 42h of continuous process is needed to realize this lift-off. The last step is the etching back of the 2 µm residual diamond substrate (see figure 1e) with an Ar/O_2 plasma in a Physical Vapour Deposition (PVD) system with magnetron sputtering. The magnetic field enhancing sputtering yield was blocked with thick mu-metal layer and the diamond sample was placed at the sputtering target place. The following parameters were set during the process: gas flows of 32 sccm for both Ar and O_2, pressure of 11.2 mbar, RF power of 200 W and DC bias of 1200 V. For these parameters, the diamond etching rate was about 1 µm/h. A first etching was stopped at a few hundred of nanometers into the residual substrate before the P-/P+/P- structure. A second etching allows stopping in the ~~1~~^{rst} first P- layer (partially etched layer), before a few hundred of nanometers of the P+/P- diamond layers. After each etching steps, SIMS measurements were carried out from the back side of the sample.

The previous steps increase the difficulty in handling together with a sample thinning. The sample size goes from a square of 3x3x0.3 mm^3 to an isosceles triangle with ~2 mm in side and ~40 µm thick. The surface morphology of both front and back sides was investigated by Atomic Force Microscopy (AFM). A Molecular Imaging PicoLE AFM was used in contact mode. The roughness average value (RMS) of the diamond surface was systematically estimated from topographic AFM images. The RMS of the front side (1.5 nm) and of the back side (2.0 nm) measured on 5x5 μm^2 surfaces are comparable (see figure 2). As boron-doped delta-layer in diamond sample (P-/P+/P- structure) presents a similar roughness on both sides, the roughness effect taking place during the SIMS sputtering might be identical for all the following SIMS results.

2.2. SIMS parameters

Secondary Ion Mass Spectrometry (SIMS) has been performed in order to measure the depth distribution of the boron concentration [B]. Specific care was taken to reach a vacuum limit of ~10^{-8} mbar in the analysis chamber. We use a CAMECA IMS4f equipment. The depth of the resulting 150x150 µm² SIMS crater was measured using a Dektak8 step-meter. The analysed zone is restricted to a diameter of 33 µm to limit the crater edge effects. The secondary ions of masses 12 (carbon) and 11 (boron) were detected. The analysis have been done at a low mass resolution, $M/\Delta M = 300$, to have a maximum sensitivity.

As the SIMS technique is mostly used in diamond to detect impurities like hydrogen or boron, measurements are performed by using parameters allowing high sensitivities. Namely the Cs^+/M- configuration is classically employed (positive primary ions with a Cs^+ source and detection of negative secondary ions of mass M). The energy of the Cs^+ primary beam is set to 10 keV. Secondary ions are detected in the negative mode (the sample is biased to -4500 V) leading to an interaction energy of the primary ions of 14.5 keV and an incidence angle of 27° with respect to the normal of the sample. Note that SIMS analysis of diamond is usually performed from the front side of the sample.

Figure 3 shows an example of the boron distribution in the P-/P+/P- diamond structure extracted from our SIMS analysis from the front side. We have plotted the boron depth profile of the P+ delta-layer (≤ 7 nm) sandwiched between two low boron doped diamond layers (P-). We observe that the sensitivity reaches four decades on the intensity. The up slope, Λ_{up}, characterises the interface between the second P- layer and the P+ layer while the down slope, Λ_{down}, characterises the interface between the P+ layer and the first P- layer (front of boron

incorporation during growth). The front and back side analyses allow estimating the stop and the onset of boron incorporation in diamond during growth of the delta-layer structure, respectively. In the following, we will study these two slopes.

The interaction mechanisms are governed by the kinetic energy, the ion nature and the incidence angle of the primary beam. As diamond analysis requires high sensitivity for impurity detection, our SIMS analysis conditions optimize the sensitivity at the expense of the depth resolution. In this study, the current of the Cs^+ ion beam is set at 40 nA allowing a sputtering rate of 0.2 nm/s.

3. Results and discussion

Figure 3 shows the boron depth profiles of our boron-doped delta-layer in diamond for the front side analysis (classical way of measurement). We observe that the delta-layer peak position is located at 335 nm in depth. The delta-layer presents an up slope, Λ_{up}, of 2.5 nm per decade (nm/dec) and a down slope, Λ_{down}, of 7.3 nm/dec. Those values are significantly different: Λ_{up} is ~3 times lower than Λ_{down}. For this analysis, Λ_{up} characterises the interface between the second P- layer and the delta-layer. This value is in agreement with our recent report [14]. Such a low value suggests that the stop of the boron doping during growth is particularly efficient.

Figure 4 shows the boron depth profiles of the boron-doped diamond delta-layer for the two intermediate back side analyses: after the first etching with a few hundred nanometers of residual diamond substrate and after the second etching with partially etched first P- layer (figure 1 e). The delta-layer peak positions of the two back side analyses are 574 nm and 238

nm in depth for the first and the second etchings respectively. The delta-layer presents an up slope, Λ_{up}, of 4.5 and 5.8 nm/dec and a down slope, Λ_{down}, of 7.6 and 8.1 nm/dec for the first and second etchings respectively. We observe that Λ_{up} values are close to 5 nm/dec. It represents the interface quality between the first P- layer and the delta-layer. This Λ_{up} denotes a good control of the front of boron incorporation during growth. The sharpness of the boron delta-layer interfaces confirms the good quality of the boron-doped delta-layer in diamond.

We observe that the delta peak position of the front side analysis is between the values of the two front side analysis (238 nm < 335 nm< 574 nm). Ideally, the precise way to compare the delta layer from the front and back side analysis would be to have the position of the delta layer at the same depth from the sample surface in each case. However, diamond etching is difficult to control at tens nm level. As a result, the position of the delta-layer is different from an etched sample to the other. Nevertheless, the boron depth profiles after the first and the second etchings present delta-layer peak positions (back side SIMS analysis) that frame the delta-layer peak position of the front side SIMS analysis. Thus it is possible to directly compare the profiles of front and back side SIMS analysis.

In figure 5, we superimpose the profile of the front side analysis to each profile of the back side analysis. The position of the delta-layer is shifted by -239 nm and +97 nm for the profile analysis of the back side after the first and the second etchings respectively. We observe that the down slopes, Λ_{down}, superimpose perfectly. On the contrary, the up slopes, Λ_{up}, differ significantly. The lowest Λ_{up} value is reached with the front side SIMS analysis (2.5 nm/dec). The slopes of the delta-layer peak plotted in figures 3 and 4 are reported in Table 2. We remind here that for the front side analysis, the Λ_{up} and Λ_{down} slopes represent the interfaces between the delta-layer and the second P- layer and between the delta-layer and the first P-

layer, respectively. Conversely, for the back side analysis, the Λ_{up} and Λ_{down} slopes represent the interfaces between the delta-layer and the first P- layer and between the delta-layer and the second P- layer, respectively.

The Λ_{down} values are all in the range of 7.5 nm/dec. According to AFM measurements (Figure 2), the roughness effect occurring during the sputtering might be identical whatever the analysed side. The similar values of Λ_{down} are explained by the fact that primary ions interact with sample atoms. A collision cascade develops in the material during the sputtering process. In our case, this effect occurs in about 10 nm in depth according to mixing-roughness-information depth (MRI) model [14, 25]. This leads to the implantation of boron atoms from the delta-layer into the neighbouring sputtered P- layer. This phenomenon is the so called "ion mixing".

The interface between the second P- layer and the P+ layer of the delta-layer structure is characterized by (i) the up slope of the front side SIMS analysis and (ii) the down slope of the back side the SIMS analysis. The values are 2.5 nm/dec for the front side analysis and systematically in the range of 7.5 nm/dec for the back side analysis. Such increase between the front and back side values clearly shows that the last value is due to an instrumental limit. Such limit is inherent to the SIMS technique. It restricts the correct description of the front of boron incorporation in the direction P-/P+ (first P- layer/delta-layer structure) for classical SIMS analysis performed from the front side of the sample. This effect was supported by our previous comparison between old and new generation of CAMECA IMS equipments (namely IMS4f and IMS7f respectively) on the SIMS characterization of the same P- / P+ / P- multilayer. Indeed, the use of lighter ions with lower kinetic energy (O_2^+ ions at 2 keV,

unreachable with a CAMECA IMS4f equipment) led to a lower Λ_{down} value due to the reduction of ion mixing (4 nm/dec instead of 7 nm/dec) [14].

4. Conclusion

In standard SIMS analysis, the measurement is performed from the surface to the substrate (front side). The depth resolution is sensitive to the burial depth of the delta-layer: the delta-layer should be as closer as possible to the sample surface. As a result, the only significant measurement in a delta-layer structure is the up slope giving access to the interface between the delta-layer and the second P- layer. In the present study, the use of a lift-off process allows to perform depth profiles of boron concentration from the substrate to the surface (back side). We have shown that the front of boron incorporation (interface between the first P- layer and delta layer) is steeper than suggested by classical SIMS analysis performed from the front side of the sample. We observe sharp interfaces of the delta layer on both sides. According to MRI model [25], we evidence the ion mixing occurring in about a depth of 10 nm in classical diamond SIMS analysis (front side). Moreover, nowadays commercialized SIMS equipment has better specifications (impact energy as low as 500 eV). In the future, the use of lighter incident ions and /or lower kinetic energy should allow a better understanding of the physical phenomena occurring during the SIMS analysis of diamond delta-layer structures. The synthesis of boron-doped delta-layers in diamond is now well controlled. As a result, it is now possible to compare boron-doped delta-layers in diamond to boron-doped delta-layers in silicon (under progress). Such structures could be further investigated for photonics, spintronics or electronics applications but could be also an alternative to silicon structures to allow measurements in conditions that silicon cannot tolerate.

Acknowledgement

The authors are grateful to José Alvarez for his scientific support on Raman analyses. The sample was provided thanks to the Deltadiam-ANR-08-BLAN-0195 contract.

References

[01] K. Ohno, F. J. Heremans, L. C. Bassett, B. A. Myers, D. M. Toyli1, A. C. Bleszynski Jayich, C. J. Palmstrøm and D. D. Awschalom, Engineering shallow spins in diamond with nitrogen delta-doping, Appl. Phys. Lett. 101 (2012) 082413; http://dx.doi.org/10.1063/1.4748280

[02] R. Edgington, S. Sato, Y. Ishiyama, R. Morris, R. B. Jackman and H. Kawarada, Growth and electrical characterisation of δ-doped boron layers on (111) diamond surfaces, J. Appl. Phys. 111 (2012) 033710; http://dx.doi.org/10.1063/1.3682760

[03] A. Fiori, T.N. Tran Thi, G. Chicot, F. Jomard, F. Omnès, E. Gheeraert and E. Bustarret, In situ etching-back processes for a sharper top interface in boron delta-doped diamond structures, Diam. Relat. Mater. 24 (2012) 175; http://dx.doi.org/10.1016/j.diamond.2012.01.018

[04] T. Ishikawa, K.-M. C. Fu, C. Santori, V. M. Acosta, R. G. Beausoleil, H. Watanabe, S. Shikata and K. M. Itoh, Optical and Spin Coherence Properties of Nitrogen-Vacancy Centers Placed in a 100 nm Thick Isotopically Purified Diamond Layer, Nano Lett. 14 (2012) 2083; http://dx.doi.org/10.1021/nl300350r

[05] H. Umezawa, M. Nagase, Y. Kato and S.-I. Shikata, High temperature application of diamond power device, Diam. Relat. Mater. 24 (2012) 201; http://dx.doi.org/10.1016/j.diamond.2012.01.011

[06] S. Yamasaki, E. Gheeraert and Y. koide, Doping and interface of homoepitaxial diamond for electronic applications, MRS Bulletin 39 (2014) 499; http://dx.doi.org/10.1557/mrs.2014.100

[07] R.S. Balmer, I. Friel, S.M. Woollard, C.J.H. Wort, G.A. Scarsbrook, S.E. Coe, H. El-Hajj, A. Kaiser, A. Denisenko, E. Kohn and J. Isberg, Unlocking diamond's potential as an electronic material, Phil. Trans. R. Soc. A 366 (2008) 251; http://dx.doi.org/0.1098/rsta.2007.2153

[08] A. Denisenko and E. Kohn, Diamond power devices. Concepts and limits, Diam. Relat. Mater. 14 (2005) 491; http://dx.doi.org/10.1016/j.diamond.2004.12.043

[09] A. Fiori, J. Pernot, E. Gheeraert and E. Bustarret, Simulations of carrier confinement in boron δ-doped diamond devices, Phys. Stat. Sol. A 207 (2010) 2084; http://dx.doi.org/10.1002/pssa.201000062

[10] G. Chicot, A. fiori, P. N. Volpe, T. N. Tran Thi, J. C. Gerbedoen, J. Bousquet, M. P. Alegre, J. C. Pinero, D. Araujo, F. Jomard, A. soltani, J. C. de Jaeger, J. Morse, J. Härtwig, N. Tranchant, C. Mer-Calfati, J. C. Arnault, J. Delahaye, T. Grenet, D. eon, F. omnès, J. Pernot and E. Bustarret, Electronic and physico-chemical properties of nanometric boron delta-doped diamond structures, J. Appl. Phys. 116 (2014) 083702; http://dx.doi.org/10.1063/1.4893186

[11] E. Kohn and A. Denisenko, Concepts for diamond electronics, Thin Sol. Films 515 (2007) 4333; http://dx.doi.org/10.1016/j.tsf.2006.07.179

[12] H. El-Hajj, A. Denisenko, A. Bergmaier, G. Dollinger, M. Kubovic and E. Kohn, Characteristics of boron δ-doped diamond for electronic applications, Diam. Relat. Mater. 17 (2008) 409; http://dx.doi.org/10.1016/j.diamond.2007.12.030

[13] P. N. Volpe, N. Tranchant, J. C. Arnault, S. Saada, F. Jomard and P. Bergonzo, Ultra-sharp boron interfaces for delta doped diamond structures, Phys. Stat. Sol. RRL 6 (2012) 59; http://dx.doi.org/10.1002/pssr.201105480

[14] C. Mer-Calfati, N. Tranchant, P.N. Volpe, F. Jomard, S. Weber, P. Bergonzo and J.C. Arnault, Sharp interfaces for diamond delta-doping and SIMS profile modelling, Mat. Lett. 115 (2014) 283; http://dx.doi.org/10.1016/j.matlet.2013.10.053

[15] A. L. Vikharev, A. M. Gorbachev, M. A. Lobaev, A. B. Muchnikov, 1, D. B. Radishev, V. A. Isaev, V. V. Chernov, S. A. Bogdanov, M. N. Drozdov and J. E. Butler, Novel microwave plasma-assisted CVD reactor for diamond delta doping, Phys. Stat. Sol. RRL 10 (2016) 324–327; http://dx.doi.org/10.1002/pssr.201510453

[16] S. Hayashi, A. Takano, H. Takenaka and Y. Homma, SIMS study of depth profiles of delta-doped boron/silicon alternating layers by low-energy ion beams, Appl. Surf. Sci. 203-204 (2003) 298; http://dx.doi.org/10.1016/S0169-4332(02)00663-3

[17] A. Takano, Y. Homma, Y. Higashi, H. Takenaka, S. Hayashi, K. Goto, M. Inoue and R. Shimizu, Evaluation of SIMS depth resolution using delta-doped multilayers and mixing–roughness-information depth model, Appl. Surf. Sci. 203–204 (2003) 294; http://dx.doi.org/10.1016/S0169-4332(02)00662-1

[18] G. Bilger, P.O. Grabitz and A. Strohm, Copper–indium–gallium–diselenide/molybdenum layers analyzed by corrected SIMS depth profiles, Appl. Surf. Sci. 231–232 (2004) 804; http://dx.doi.org/10.1016/j.apsusc.2004.03.077

[19] F. Laugiera, J.M. Hartmann, H. Moriceau, P. Holliger, R. Truche and J.C. Dupuy, Backside and frontside depth profiling of B delta doping, at low energy, using new and previous magnetic SIMS instruments, Appl. Surf. Sci. 231–232 (2004) 668; http://dx.doi.org/10.1016/j.apsusc.2004.03.143

[20] C. Hongo, M. Tomita and M. Takenaka, Accurate depth profiling for ultra-shallow implants using backside-SIMS, Appl. Surf. Sci. 231–232 (2004) 673; http://dx.doi.org/10.1016/j.apsusc.2004.03.236

[21] T. N. Tran Thi, B. Fernandez, D. Eon, E. Gheeraert, J. Härtwig, T. Lafford, A. Perrat-Mabilon, C. Peaucelle, P. Olivero and E. Bustarret, Ultra-smooth single crystal diamond

surfaces resulting from implantation and lift-off processes, Phys. Stat. Sol. A 208 (2011) 2057; http://dx.doi.org/10.1002/pssa.201100038

[22] C. Mer-Calfati, N. Habka, A. Ben-Younes, M.-A. Pinault, J. Barjon and P. Bergonzo, High surface smoothening of diamond HPHT (100) substrates, Phys. Status Solidi A, 9 (2009) 1955; http://dx.doi.org/10.1002/pssa.200982232

[23] P.-N. Volpe, J.-C. Arnault, N. Tranchant, G. Chicot, J. Pernot, F. Jomard and P. Bergonzo, Boron incorporation issues in diamond when TMB is used as precursor: Toward extreme doping levels, Diam. Relat. Mater. 22 (2012) 136; http://dx.doi.org/10.1016/j.diamond.2011.12.019

[24] M.J. Marchywka, United State Patent “Electrochemical process and product therefrom”, Family ID 25546551, Appl. No 07/999,629, December 31, 1992

[25] S. Hofmann and J. Y. Wang, he MRI-Model in Sputter Depth Profiling: Capabilities, Limitations and Recent Progress, J. Surf. Anal. 13 (2006) 142

Table captions

Table 1: Growth parameters for P-/P+/P- multilayers. The thickness and the boron content of the layers are measured by front side SIMS analysis.

Table 2: Up and down slopes of the delta structures plotted in figures 3 and 4.

Figure captions

Figure 1: Schematic realization of the P- / P+ / P- sample (five steps) with (a) the ion implantation of the HPHT (100) diamond substrate followed by (b) the growth of the delta structure for the SIMS analysis on the front side, then (c) the growth of a diamond bulk layer for handling purpose followed by (d) a lift-off and (e) an etching of the diamond substrate allowing the SIMS analysis of the back side.

Figure 2: AFM images of the sample surfaces (a) after the second step (front side) and (b) after the second etching of the 5th step (back side) of the P-/P+/P- sample.

Figure 3: SIMS profiles of 11 mass (boron) centred around the boron delta-doped diamond layer sandwiched between two low boron doped diamond layers. The profile has been performed from the front side of the sample.

Figure 4: Boron SIMS profiles of the boron delta doped diamond sample from the back side analyses performed a) after the 1^{rst} etching (with a few hundred of residual substrate) and b) after the second etching (with partially etched first P- layer).

Figure 5: Zoom in the boron SIMS profiles by overlaying the front side analysis to each back side analysis (on the left, after the first etching and on the right, after the second etching). For convenience to the eye, the delta peak positions of the back side profiles have been shifted to coincide to the one of the front side profile.

Layer	CH_4/H_2 (%)	O_2/H_2 (%)	$(B/C)_{gas}$ (ppm)	Thickness (nm)	[B] (at/cm^3)
First P-	1	0.25	Residual	320	$3x10^{16}$
P+	0.6	0	21400	≤ 7	$2x10^{20}$
Second P-	1	0.25	Residual	350	$3x10^{16}$

Table 1

		Delta position (nm)	Λ_{up} (nm/dec)	Λ_{down} (nm/dec)
Front side		335	2.5	7.3
Back side	1^{rst} etching	574	4.5	7.6
	2^{nd} etching	238	5.8	8.1

Table 2

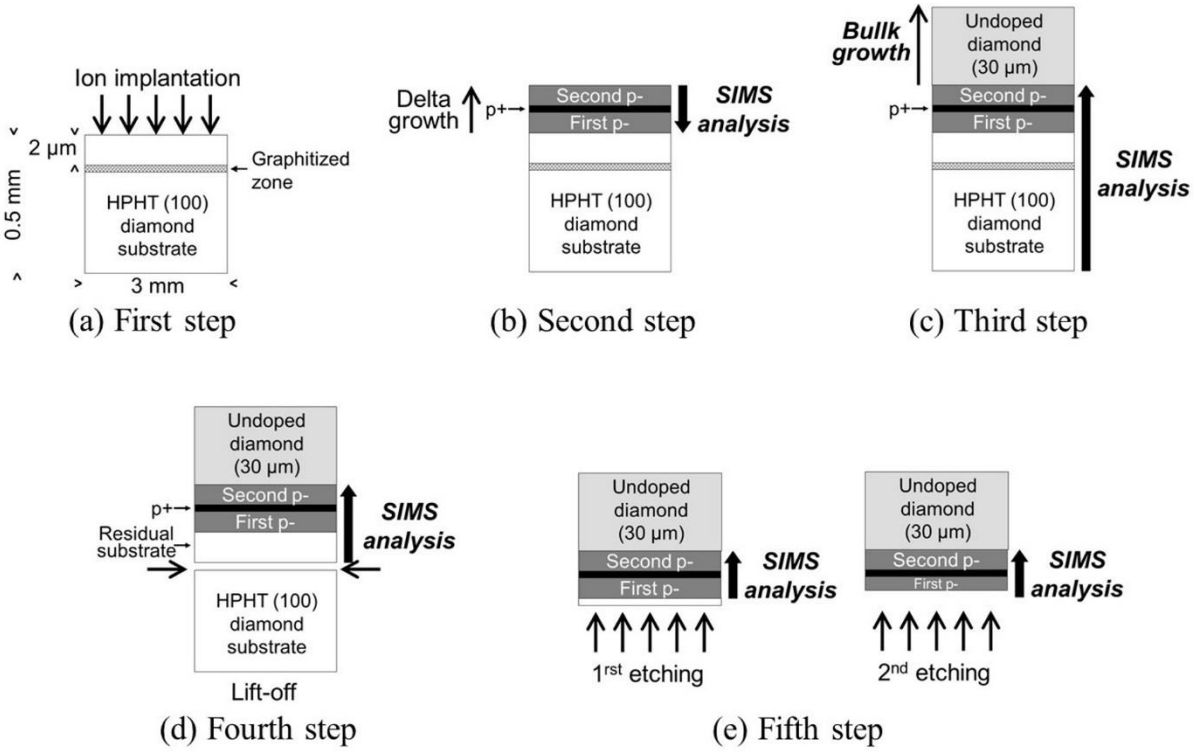
Ion implantation
2 µm
0.5 mm
3 mm
Graphitized zone
HPHT (100) diamond substrate
(a) First step
Delta growth
p+
Second p-
First p-
SIMS analysis
HPHT (100) diamond substrate
(b) Second step
Bullk growth
Undoped diamond (30 µm)
Second p-
First p-
p+
SIMS analysis
HPHT (100) diamond substrate
(c) Third step
Undoped diamond (30 µm)
p+
Second p-
First p-
Residual substrate
SIMS analysis
HPHT (100) diamond substrate
Lift-off
(d) Fourth step
Undoped diamond (30 µm)
Second p-
First p-
SIMS analysis
1rst etching
Undoped diamond (30 µm)
Second p-
First p-
SIMS analysis
2nd etching
(e) Fifth step

Figure 1

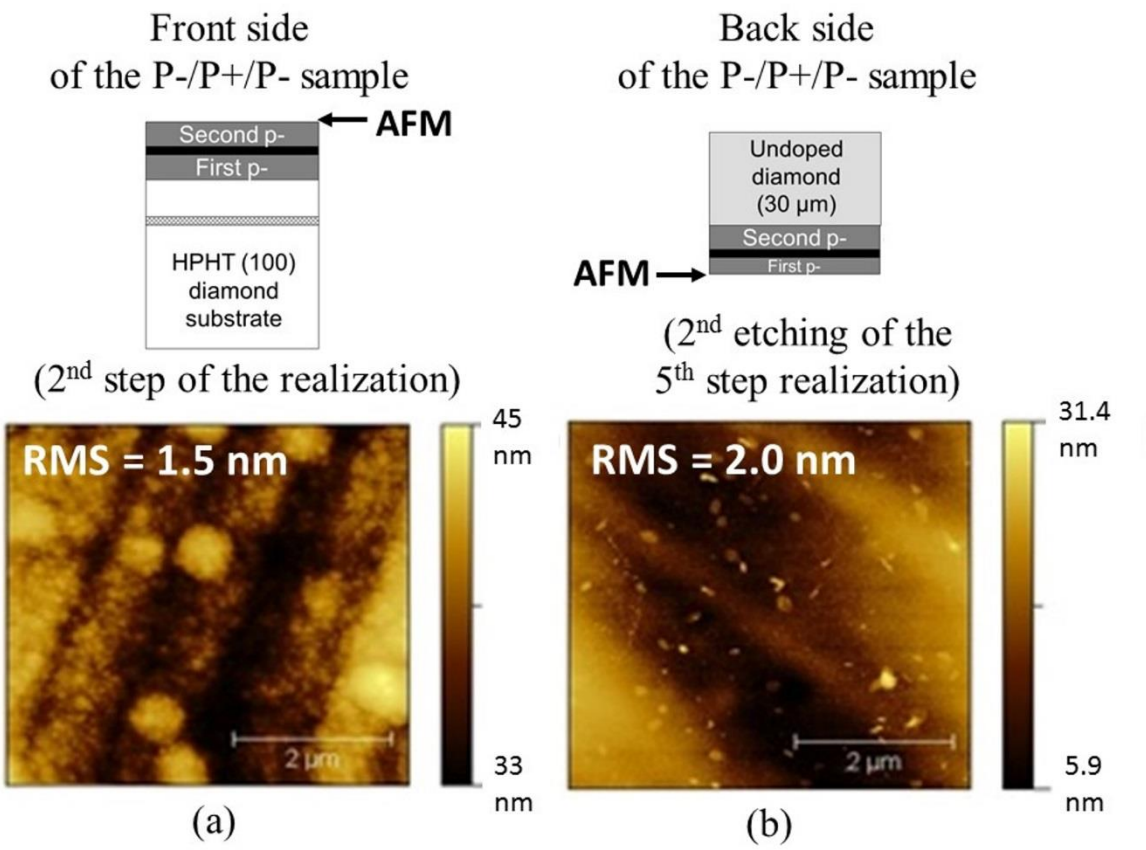
Front side
of the P-/P+/P- sample
AFM
Second p-
First p-
HPHT (100)
diamond
substrate
(2nd step of the realization)
RMS = 1.5 nm
2 µm
45
nm
33
nm
(a)
Back side
of the P-/P+/P- sample
Undoped
diamond
(30 µm)
Second p-
First p-
AFM
(2nd etching of the
5th step realization)
RMS = 2.0 nm
2 µm
31.4
nm
5.9
nm
(b)

Figure 2

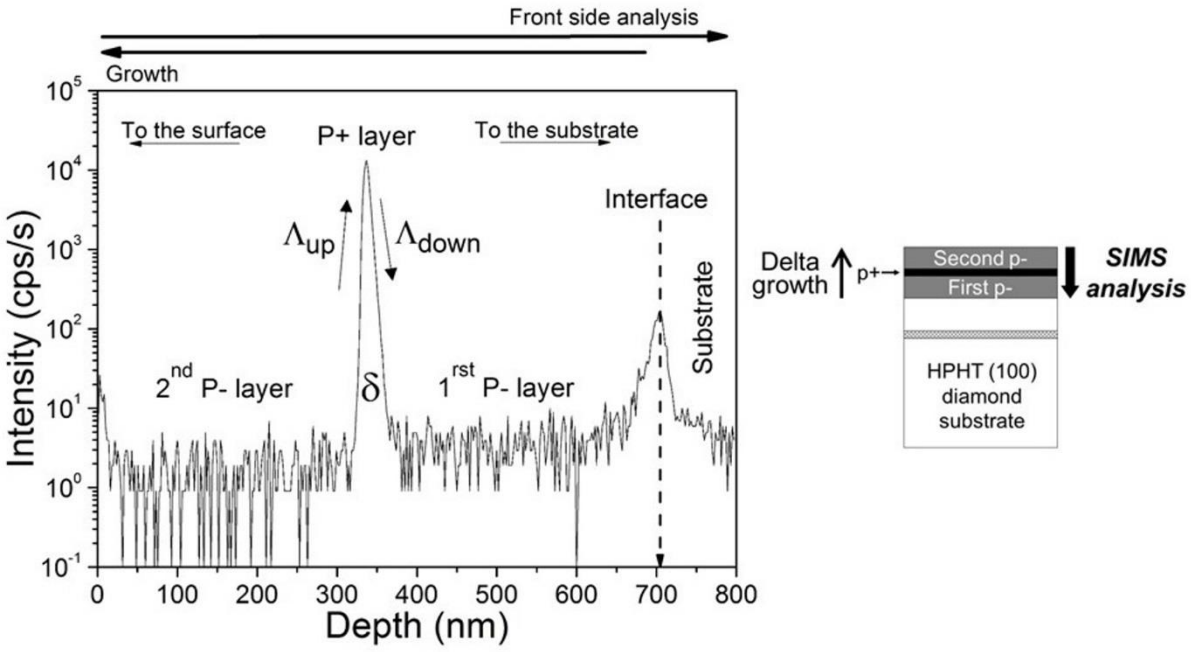
Front side analysis
Growth
To the surface
P+ layer
To the substrate
Interface
Substrate
Λ_{up}
Λ_{down}
2^{nd} P- layer
δ
1^{rst} P- layer
Intensity (cps/s)
Depth (nm)
Delta growth
p+
Second p-
First p-
SIMS analysis
HPHT (100) diamond substrate

Figure 3

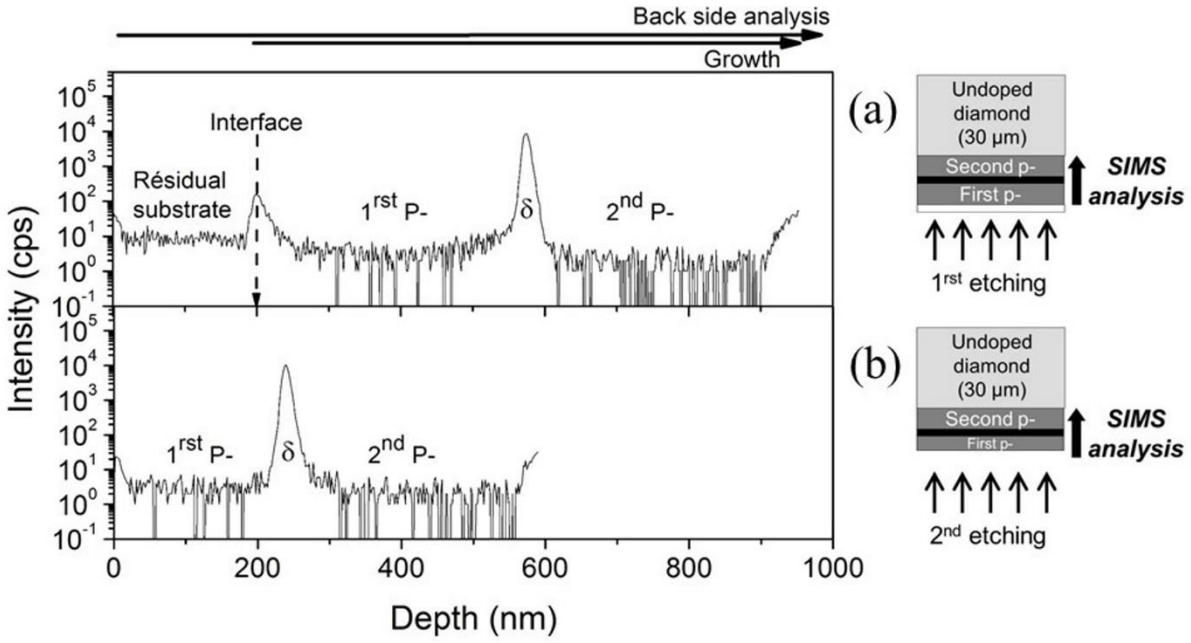
Back side analysis
Growth
Intensity (cps)
Interface
Résidual substrate
1rst P-
δ
2nd P-
(a)
(b)
Undoped diamond (30 µm)
Second p-
First p-
SIMS analysis
1rst etching
2nd etching
Depth (nm)
0
200
400
600
800
1000

Figure 4

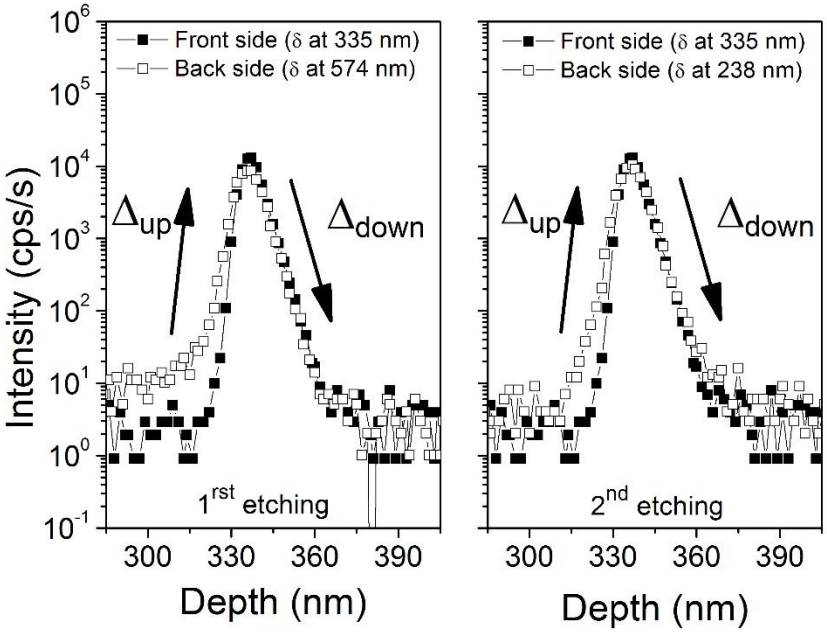
Front side (δ at 335 nm)
Back side (δ at 574 nm)
Intensity (cps/s)
Δup
Δdown
1rst etching
Depth (nm)
Front side (δ at 335 nm)
Back side (δ at 238 nm)
Δup
Δdown
2nd etching
Depth (nm)

Figure 5